



## Proposal of Electromagnetic Noise-generating Mechanism on Carrier Harmonics

Yoshitake KAMIJO<sup>1</sup>; Shun TANIGUCHI<sup>1</sup>; Makoto MATSUSHITA<sup>1</sup>

<sup>1</sup> Toshiba Corporation, Japan

### ABSTRACT

Recent traction motors are operated with the traction inverter to ensure the high efficient drive and variable drive speed. In such the application, electromagnetic harmonics noise by the carrier frequency from traction inverters occur the sound noise which are radiated from the motor surface. In the conventional method to reduce the noise by the carrier frequency, sometimes the career frequency distribution has been used to reduce the electromagnetic noise. Since the relationship between structural characteristics and electromagnetic noise are not clear, the noise reduction is limited by the career frequency distribution. To make it clear the relationship between the mechanical motor characteristics and career frequency characteristics, this paper reports the results and consideration based on the investigation for the relationship between the electromagnetic-force modes in career frequency and the natural vibration modes. The electromagnetic noise by career harmonics is described by the vibration response that is represented by the product of electromagnetic-force mode and natural vibration mode.

Keywords: Career Frequency, Characteristic Vibration Mode, Electromagnetic-force Mode  
I-INCE Classification of Subjects Number(s): 21.7

### 1. INTRODUCTION

In industrial applications, to ensure the high efficient and energy-saving drive, the traction inverters are used to drive the traction motors. The traction inverter also allows the variable speed drive. However in term of electromagnetic noise source by the traction inverter, the electromagnetic noise with side band harmonics are occurred and varied by the drive speed. The use of magnetic flux with permanent magnets enables Permanent Magnet Synchronous Motors (PMSM) to achieve higher flux, torque with higher efficiency than Asynchronous Induction Motors.

Also the weight saving of traction motors is expected to ensure the lower energy consumption in the automobile or rolling applications. Structures of PMSM tend to be designed with weight-saved case body, compared to conventional AIMs. Consequently the high electromagnetic flux density and slightly weight-saved structure are likely to have the vibration and sound noise problem.

Conventionally, career distribution was adopted in control as electromagnetic noise-control technology on carrier harmonics. However, since structure and an electromagnetic noise-generating mechanism are not known, effective distribution cannot be performed and the big effect is not acquired. Also, the motor has adopted anti-eccentric structurally, but it is ineffective for high-frequency noise.

This paper reports the generating mechanism of the noise which is investigated by the Experimental Modal Analysis measurements and FEM (Finite Elemental Method). It pays attention to the relation between the electromagnetic-force mode on career frequency, and the natural vibration mode on structure.

### 2. EXPERIMENTAL MODAL ANALYSIS

#### 2.1 Tested Motors

Figure 1 shows the schematic diagram of the tested motor in Experimental Modal Analysis. The motor consists of a rotor and stator. The stator is installed and fixed in the case. In addition, the motor is supported by bearing brackets on both sides of the case. Rotation in the motor unit can be realized.

<sup>1</sup> yoshitake.kamijo@toshiba.co.jp

Table 1 shows the specifications of the motor.

Target motors are two types. One is 4-Pole and 6-Slot (4P6S) PMSM with concentrated windings and the other is 6-Pole and 9-Slot (6P9S) PMSM with concentrated windings.

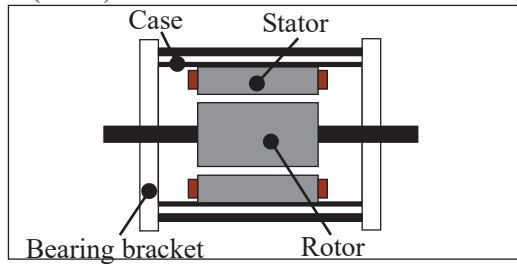


Figure 1 – Motor Structure

Table 1 – Specifications

Outer diameter of stator	$\varphi 110.52$ mm
Outer diameter of rotor	$\varphi 56.6$ mm
Core length	55 mm
Air gap	0.7 mm

## 2.2 Measured Conditions and Results (4P6S)

The twenty vibration acceleration sensors are located on the case surface. The natural frequency of stator is tested by hammering test with the impulse hammer. For validation of the harmonics, data up to 20 kHz. Figure 2 shows the natural frequency extracted from the test. 2.8 kHz is ellipse mode ( $N = 2$ ), 7.8 kHz is triangle mode ( $N = 3$ ), 10.2 kHz is rectangle mode ( $N = 4$ ), 11.2 kHz is expansion and contraction mode ( $N = 0$ ).

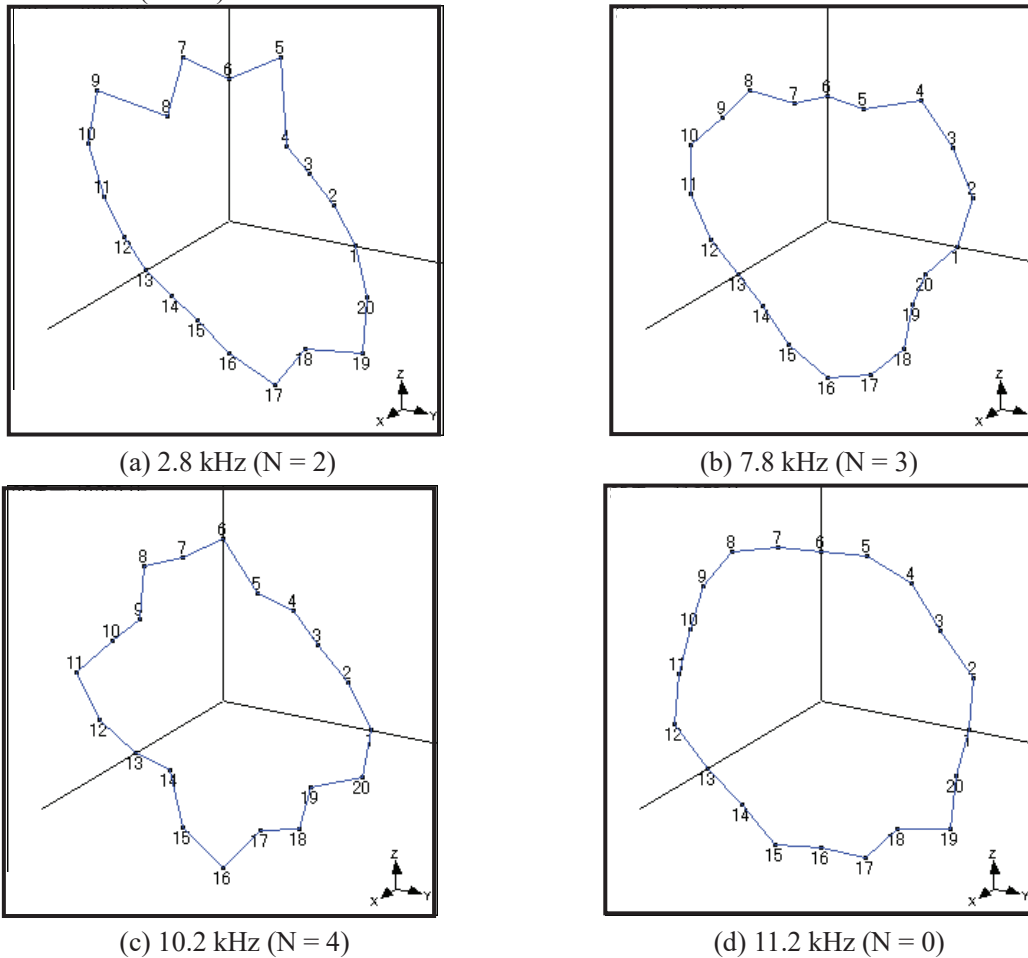


Figure 2 – Natural vibration mode (4P6S)

## 2.3 Measured Conditions and Results (6P9S)

The vibration acceleration sensors are located around the case in the range containing the rotor. The natural frequency of stator is investigated by hammering test using impulse hammer. For validation of the harmonics, it gets data up to 20 kHz. Figure 3 shows the natural frequency extracted from the test. 2.0 kHz is ellipse mode ( $N = 2$ ), 4.5 kHz is triangle mode ( $N = 3$ ), 8.1 kHz is rectangle mode ( $N = 4$ ).

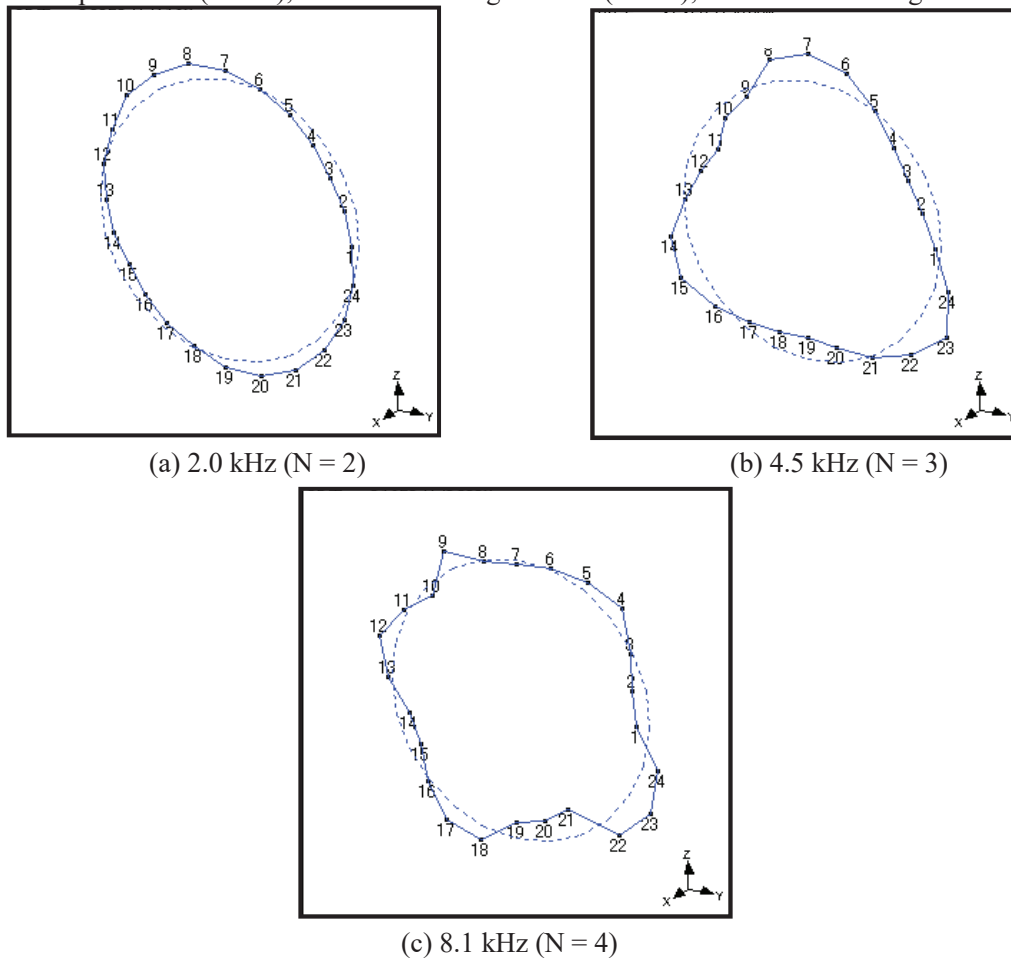


Figure 3 – Natural vibration mode (6P9S)

## 3. DRIVING TEST

### 3.1 Test Results (4P6S)

In general, the noise level is superior by resonance structures. Therefore, the noise level can be superior, matching the natural frequency of the structure to the carrier frequency. This test proposes to excite the resonance structure by carrier frequency. In theory, when the modulation rate is close to zero, twice the carrier frequency is superior by reference (1). Thus, it becomes possible to excite the resonance structure by selecting the carrier frequency to be  $1/2$  the natural frequency of the structure. The natural frequencies are 2.8 kHz ( $N = 2$ ), 7.8 kHz ( $N = 3$ ), 10.2 kHz ( $N = 4$ ) and 11.2 kHz ( $N = 0$ ). Therefore, each carrier frequency sets to 1.4 kHz, 3.9 kHz, 5.1 kHz and 5.6 kHz. To prevent the side band of the carrier frequency by rotating speed, driving frequency is 4 Hz. Figure 4 shows frequency analysis results of vibration acceleration. Carrier frequency is “cf” and driving frequency is “df”. As this results show, the principal component of the vibration acceleration is multiples of the carrier frequency. Focusing on twice the carrier frequency to excite the resonance structure, the following results are shown. When twice the carrier frequency equals to 2.8 kHz ( $N = 2$ ), 10.2 kHz ( $N = 4$ ) and 11.2 kHz ( $N = 0$ ), the vibration is superior. However, when it equals to 7.8 kHz ( $N = 3$ ), the vibration is not superior. Also, Figure 5 shows vibration mode on driving. As the results show, at 2.8 kHz ( $N = 2$ ), 10.2 kHz ( $N = 4$ ) and 11.2 kHz ( $N = 0$ ), the shape of the natural frequency mode equals to vibration mode on driving. However, at 7.8 kHz ( $N = 3$ ), natural vibration mode do not equal to vibration mode

on driving, and no mode appears. Therefore, it is said that in 4P6S PMSM with concentrated windings,  $N = 3$  disappears on driving and is not superior. Noise level is correlated with vibration acceleration level. Figure 6 shows noise level for each. The higher the vibration acceleration, noise is high.

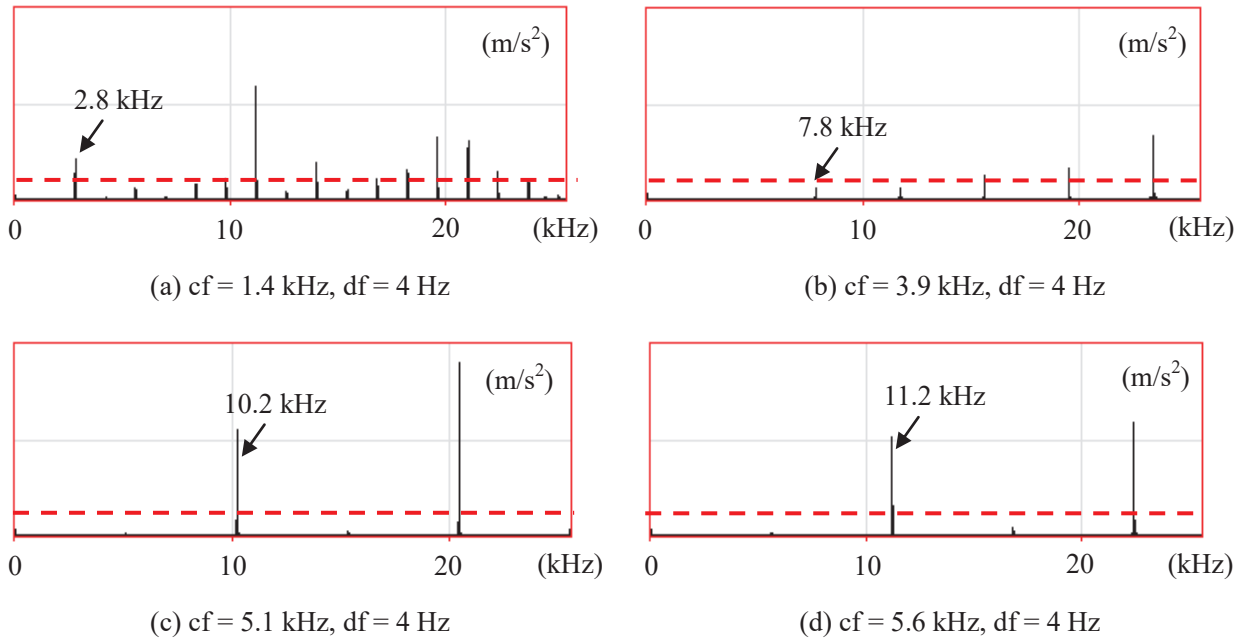


Figure 4 – Frequency analysis (4P6S)

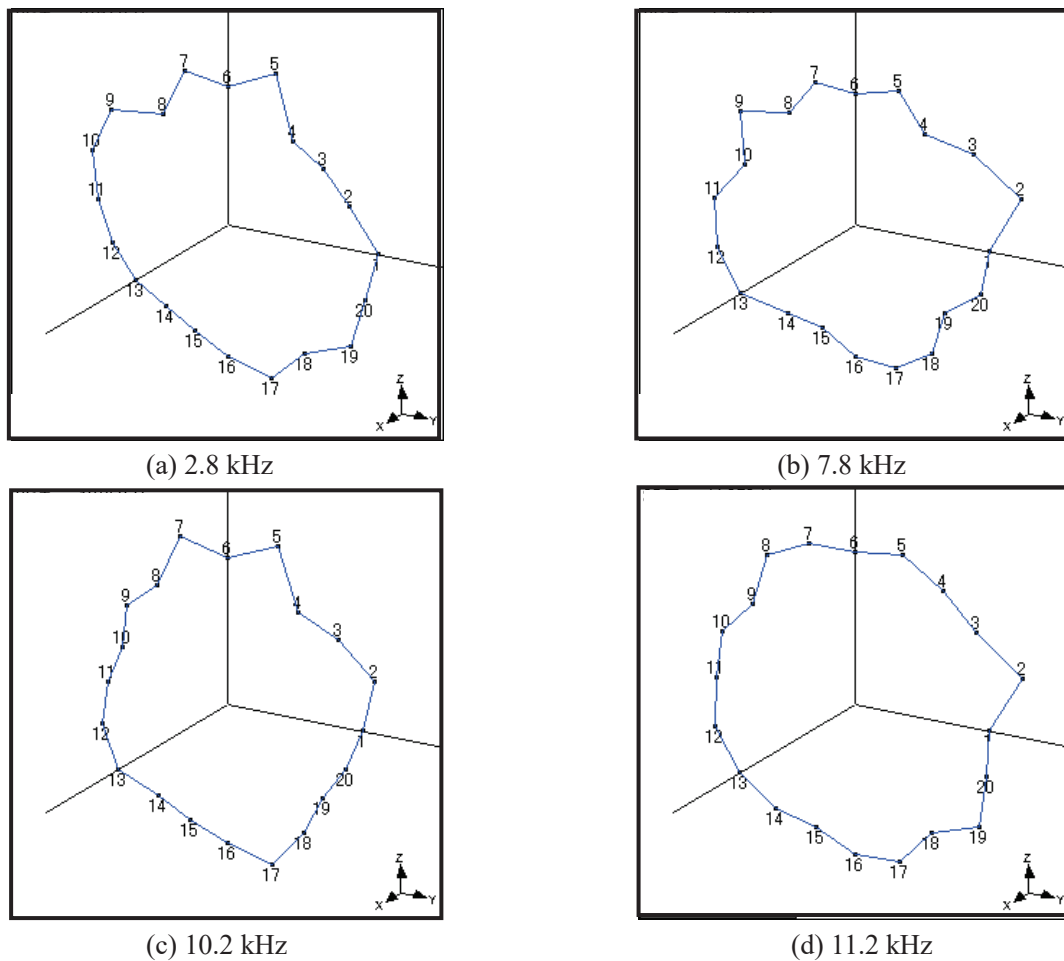


Figure 5 – Vibration mode on driving (4P6S)

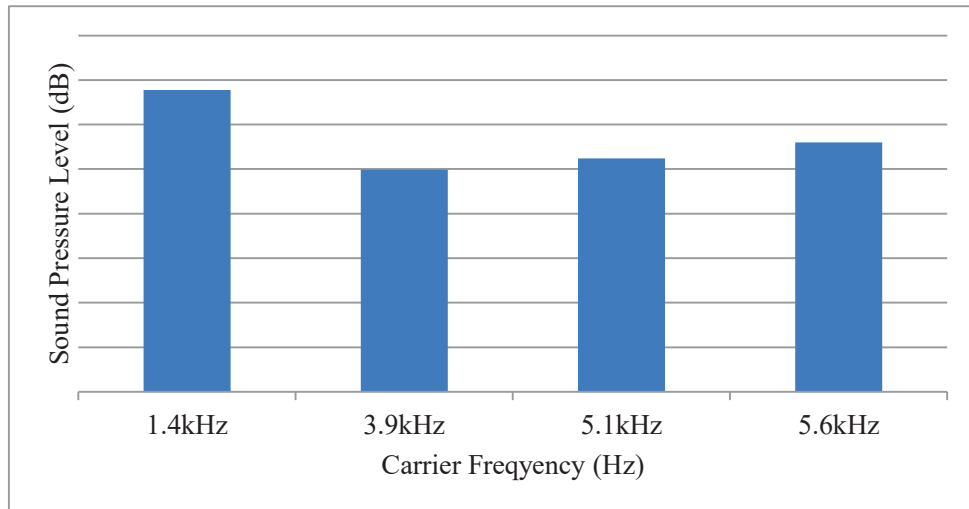


Figure 6 – Noise level (4P6S)

### 3.2 Test Results (6P9S)

As is the case with 4P6S, it becomes possible to excite the resonance structure by selecting the carrier frequency to be 1/2 the natural frequency of the structure. The natural frequencies are 2.0 kHz (N = 2), 4.5 kHz (N = 3) and 8.1 kHz (N = 4). Therefore, each carrier frequency sets to 1.0 kHz, 2.25 kHz and 4.05 kHz. To prevent the side band of the carrier frequency by rotating speed, driving frequency is the same as 4P6S. Figure 7 shows frequency analysis results of vibration acceleration. As this results show, the principal component of the vibration acceleration is multiples of the carrier frequency. Focusing on twice the carrier frequency to excite the resonance structure, the following results are shown. When twice the carrier frequency equals to 4.5 kHz (N = 3), the vibration is superior. However, when it equals to 2.0 kHz (N = 2) and 8.1 kHz (N = 4), the vibration is not superior. Also, Figure 8 shows vibration mode on driving. As the results show, at 4.5 kHz (N = 3), the shape of the natural vibration mode equals to vibration mode on driving. However, at 2.0 kHz (N = 2) and 8.1 kHz (N = 4), natural vibration mode do not equal to vibration mode on driving, and no mode appears. Therefore, it is said that in 6P9S PMSM with concentrated windings, N = 2 and N = 4 disappear on driving and are not superior. Figure 9 shows noise level for each. The higher the vibration acceleration, noise is high.

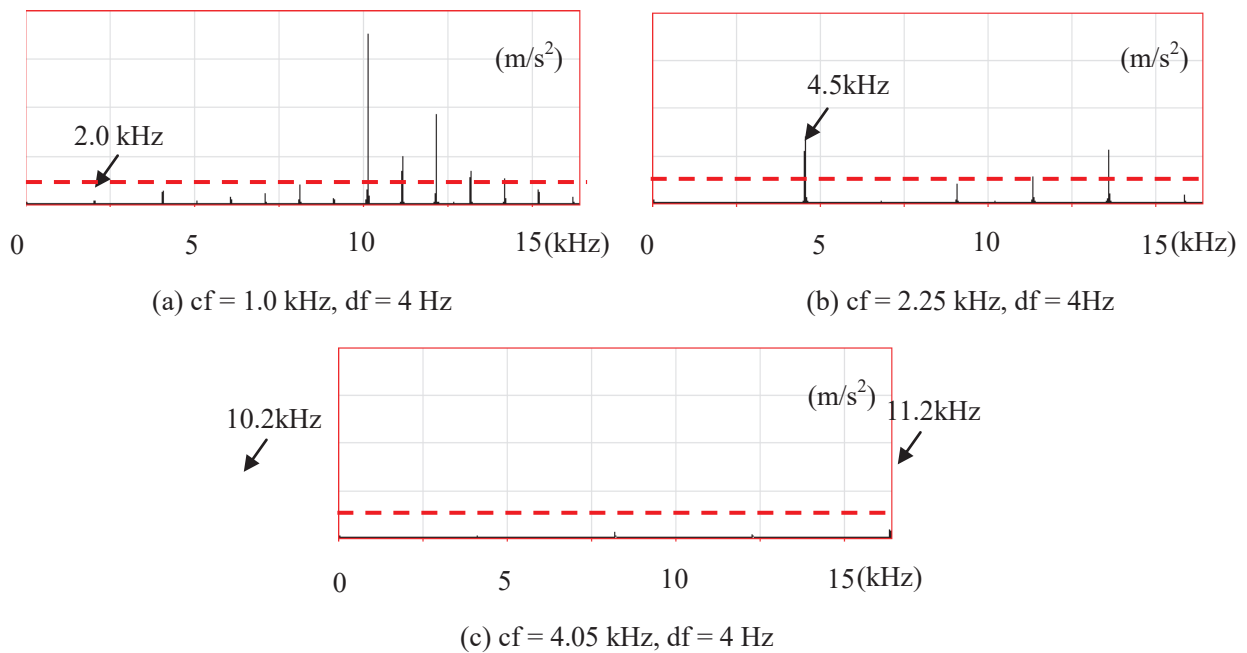
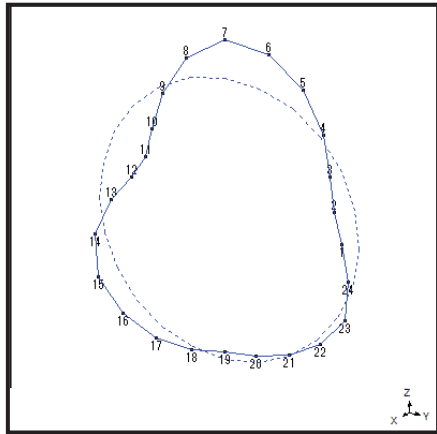
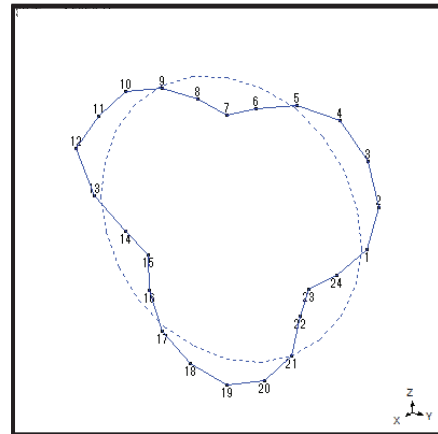


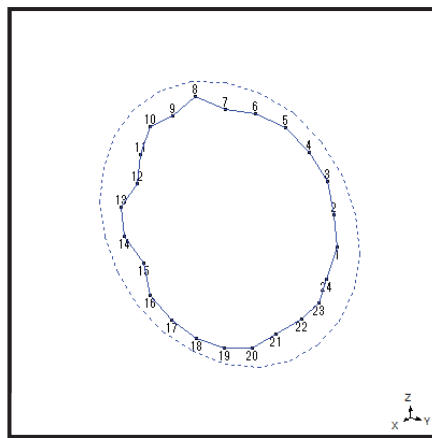
Figure 7 – Frequency analysis (6P9S)



(a) 1.0 kHz



(b) 2.25 kHz



(c) 4.05 kHz

Figure 8 – Vibration mode on driving (6P9S)

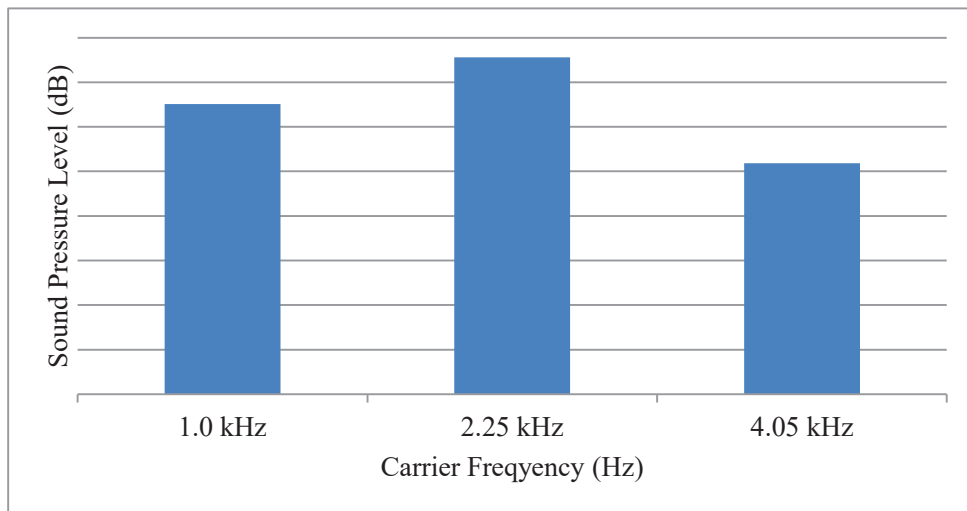


Figure 9 – Noise level (6P9S)

## 4. MECHANISM OF ELECTROMAGNETIC NOISE ON HARMONICS

### 4.1 Electromagnetic-Structure Interaction Analysis

Electromagnetic force propagated from the rotor to the stator has several modes as well as the natural frequency of the structure. In the case of the 4-pole motor, electromagnetic force modes ( $M$ ) could be  $M = 0$ ,  $M = 2$  and  $M = 4$ . Each of these is expansion and contraction mode, ellipse mode and rectangle mode. FEM analysis is made by giving electromagnetic force distribution with these electromagnetic modes on the stator teeth. Figure 10 shows how to give the electromagnetic force. The analysis results of  $M = 0$  and  $M = 2, 4$  are shown in Figure 11 and Figure 12. In the case of  $M = 0$ ,  $N = 2$ ,  $N = 3$  and  $N = 4$  do not appear and  $N = 0$  is superior. In the case of  $M = 2$  or  $M = 4$ ,  $N = 3$  and  $N = 0$  do not appear and  $N = 2, 4$  are superior.  $N = 3$  has disappeared in any case. This denotes the same tendency of measurement results. Distributed windings are likely to be close to the former case.

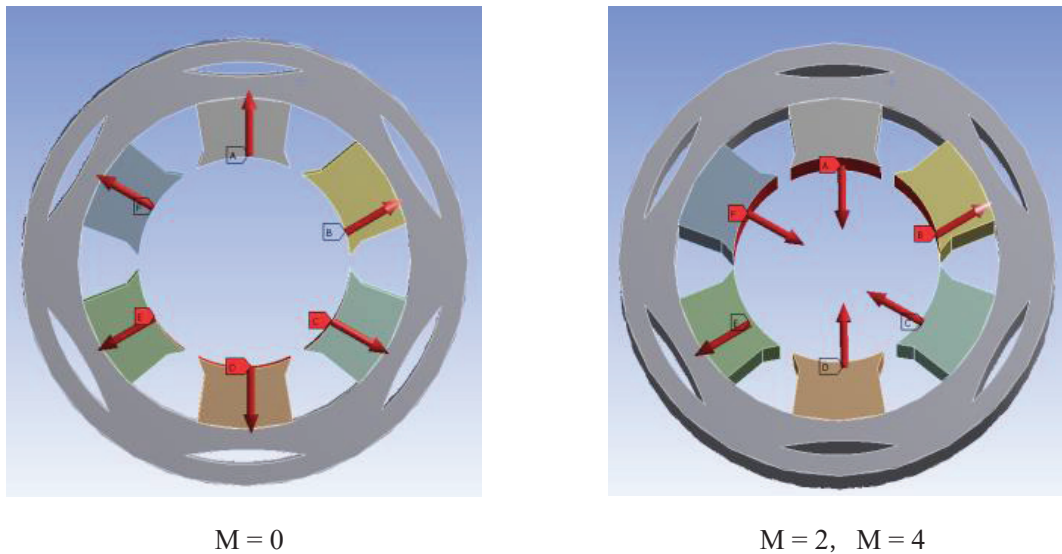


Figure 10 – Electromagnetic force condition

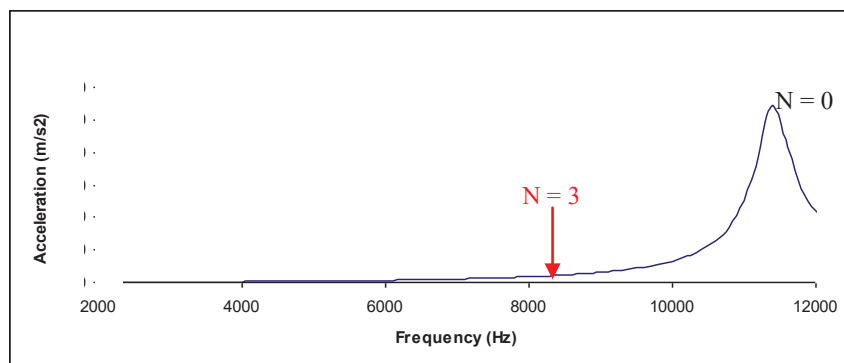


Figure 11 – Response analysis result on  $M=0$

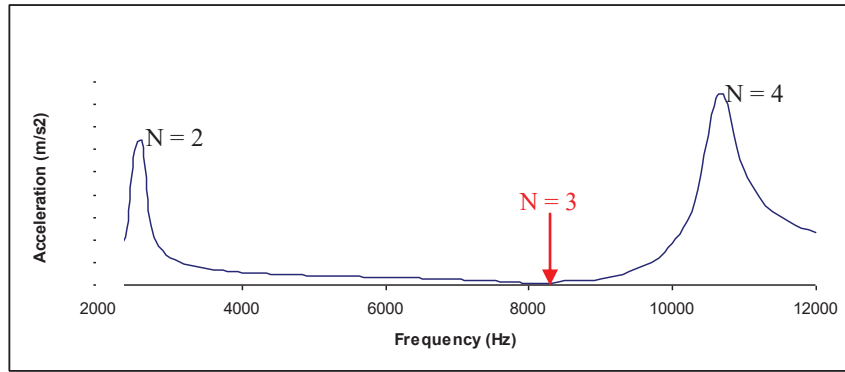


Figure 12 – Response analysis result on M=2, M=4

#### 4.2 Formulation of the Theory

This paper proposes the mechanism of electromagnetic noise on carrier harmonics with measurement and analysis. The general solution is derived from these results. This paper holds 4P6S up as an example.

Figure 13 shows the natural vibration mode. Each mode represented by a matrix as follows.

$$N = 2 \Rightarrow (1 \quad -1 \quad -1 \quad 1 \quad -1 \quad -1)$$

$$N = 3 \Rightarrow (1 \quad -1 \quad 1 \quad -1 \quad 1 \quad -1)$$

$$N = 4 \Rightarrow (1 \quad -1 \quad -1 \quad 1 \quad -1 \quad -1)$$

$$N = 0 \Rightarrow (1 \quad 1 \quad 1 \quad 1 \quad 1 \quad 1)$$

Where plus (+) is outward-directed, minus (-) is inward-directed.

Each electromagnetic force mode represented by a matrix as follows.

$$M = 0 \Rightarrow \begin{pmatrix} 1 \\ 1 \\ 1 \\ 1 \\ 1 \\ 1 \end{pmatrix}, M = 2 \Rightarrow \begin{pmatrix} 1 \\ -1 \\ -1 \\ 1 \\ -1 \\ -1 \end{pmatrix}, M = 4 \Rightarrow \begin{pmatrix} 1 \\ -1 \\ -1 \\ 1 \\ -1 \\ -1 \end{pmatrix}$$

As above, Vibration response (Z) is calculated by multiplying the natural vibration mode by the electromagnetic force mode as follows.

$$\begin{aligned} &\text{Natural vibration mode (N)} \times \text{Electromagnetic force mode (M)} \\ &= \text{Vibration response (Z)} \begin{cases} Z \leq 0 & \text{disappear} \\ Z > 0 & \text{appear} \end{cases} \end{aligned}$$

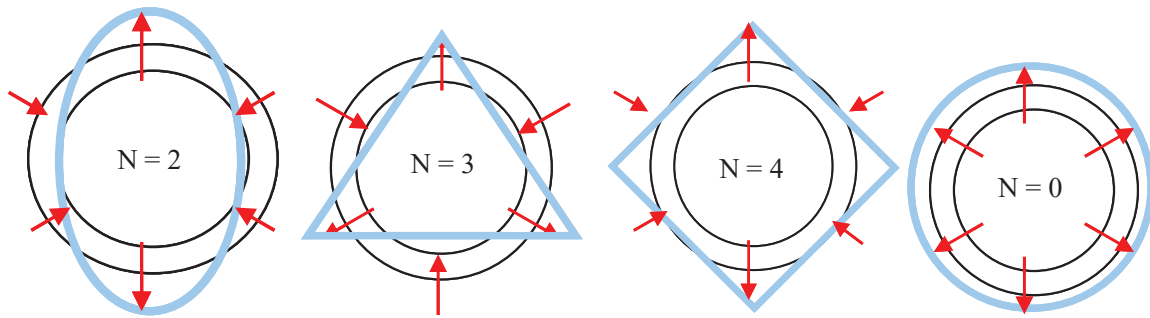


Figure 13 – Natural vibration mode (N)

## 5. CONCLUSIONS

This paper reports the generating mechanism of the noise which is explained by the experimental result and FEM analysis for the vibration and noise. As the interaction of natural vibration modes (N) and electromagnetic force carrier (M), N = 3 is disappeared in case of 4P6S. N = 2 and N = 4 are disappeared in case of 6P9S. The electromagnetic noise generated by carrier harmonics may be represented by the reciprocal amplification phenomena with natural vibration modes and electromagnetic force modes.

## REFERENCES

1. Research Committee on Semiconductor Power Converter System (Institute of Electrical Engineers of Japan) Semiconductor Power Converter Circuit; 1987. p. 113-126.